Integrated Transcriptomic and Metabolomic Characterization of the Low-Carbon Response Using an *ndhR* Mutant of *Synechocystis* sp. PCC 6803[1]

Stephan Klähn, Isabel Orf, Doreen Schwarz, Jasper K.F. Matthiessen, Joachim Kopka, Wolfgang R. Hess, and Martin Hagemann*

Genetics and Experimental Bioinformatics, Institute of Biology III, University of Freiburg, D–79104 Freiburg, Germany (S.K., J.K.F.M., W.R.H.); Max-Planck-Institute of Molecular Plant Physiology, Department of Molecular Physiology: Applied Metabolome Analysis, D–14476 Potsdam-Golm, Germany (I.O., J.K.); and Plant Physiology Department, Institute of Biological Sciences, University of Rostock, D–18059 Rostock, Germany (D.S., M.H.)

The acquisition and assimilation of inorganic carbon (Ci) represents the largest flux of inorganic matter in photosynthetic organisms; hence, this process is tightly regulated. We examined the Ci-dependent transcriptional and metabolic regulation in wild-type *Synechocystis* sp. PCC 6803 compared with a mutant defective in the main transcriptional repressor for Ci acquisition genes, the NAD(P)H dehydrogenase transcriptional regulator NdhR. The analysis revealed that many protein-coding transcripts that are normally repressed in the presence of high CO_2 (HC) concentrations were strongly expressed in Δ*ndhR*, whereas other messenger RNAs were strongly down-regulated in mutant cells, suggesting a potential activating role for NdhR. A conserved NdhR-binding motif was identified in the promoters of derepressed genes. Interestingly, the expression of some NdhR-regulated genes remained further inducible under low-CO_2 conditions, indicating the involvement of additional NdhR-independent Ci-regulatory mechanisms. Intriguingly, we also observed that the abundance of 52 antisense RNAs and 34 potential noncoding RNAs was affected by Ci supply, although most of these molecules were not regulated through NdhR. Thus, antisense and noncoding RNAs could contribute to NdhR-independent carbon regulation. In contrast to the transcriptome, the metabolome in Δ*ndhR* cells was similar to that of wild-type cells under HC conditions. This observation and the delayed metabolic responses to the low-CO_2 shift in Δ*ndhR*, specifically the lack of transient increases in the photorespiratory pathway intermediates 2-phosphoglycolate, glycolate, and glycine, suggest that the deregulation of gene expression in the Δ*ndhR* mutant successfully preacclimates cyanobacterial cells to lowered Ci supply under HC conditions.

The acquisition and fixation of inorganic carbon (Ci) during photosynthesis generates an estimated net fixation of 210 gigatons of carbon per year (Stuart, 2011), representing the largest nutrient flux in living cells. Ci availability is often considered a limiting factor for photosynthetic performance. For example, in marine environments, the typical Ci level is constantly low at approximately 2 mM (Price et al., 2008). The central enzyme for photosynthetic carbon fixation is Rubisco, which catalyzes the carboxylation of ribulose-1, 5-bisphosphate (RubP), generating two molecules of 3-phosphoglycerate. As the evolutionary ancestors of all eukaryotic chloroplasts (Ochoa de Alda et al., 2014), cyanobacteria constitute the prokaryotic model for Ci acquisition. These organisms also represent a globally important CO_2 sink and are significant primary producers.

The cyanobacterial Rubisco is adapted to the elevated CO_2 concentrations prevalent in the ancient atmosphere more than 350 million years ago (Berner, 1990). This apparent defect results in a rather low affinity for CO_2 compared with Rubisco in algae or land plants (Price et al., 2008). To ensure efficient carbon fixation in the present-day CO_2-poor environment, cyanobacteria developed a carbon-concentrating mechanism (CCM). The CCM includes efficient carbon uptake systems and the enrichment of CO_2 around Rubisco caged within the carboxysome. Furthermore, the CCM apparently minimizes another limitation of Rubisco (i.e. the use of oxygen instead of CO_2 as a

[1] This work was supported by the Deutsche Forschungsgemeinschaft (grant no. HA2002/8–3 and Research Unit FOR 1186, PROMICS to J.K. and M.H.) and by the Federal Ministry for Education and Research (CYANOSYS grant no. 0316183 to J.K., W.R.H., and M.H.).

* Address correspondence to martin.hagemann@uni-rostock.de.

The author responsible for distribution of materials integral to the findings presented in this article in accordance with the policy described in the Instructions for Authors (www.plantphysiol.org) is: Martin Hagemann (martin.hagemann@uni-rostock.de).

D.S. and M.H. conceived the original research plans; J.K., W.R.H., and M.H. supervised the experiments; D.S. performed the growth experiments and the sampling; S.K. and J.K.F.M. performed the transcriptomics and promoter analyses; I.O. performed the metabolome analyses; M.H., S.K., W.R.H., and J.K. designed the experiments; S.K. and I.O. performed the integrated data analysis; M.H., S.K., W.R.H., and J.K. conceived the project and wrote the article with contributions of all the authors; M.H. coordinated and complemented the writing.

www.plantphysiol.org/cgi/doi/10.1104/pp.114.254045

substrate in the oxygenase reaction; Hackenberg et al., 2011). The resulting by-product, 2-phosphoglycolate (2PG), is toxic to photoautotrophic cells, because 2PG inhibits Calvin-Benson cycle enzymes (Kelly and Latzko, 1977; Husic et al., 1987; Norman and Colman, 1991). To metabolize 2PG, all oxygenic phototrophs evolved the photorespiratory 2PG metabolism (Bauwe et al., 2010). Multimodal 2PG metabolism, including the canonical photorespiratory cycle active in land plants, is essential for growth under ambient air conditions among cyanobacteria, indicating that the CCM is insufficient to completely suppress the oxygenase function of Rubisco (Eisenhut et al., 2008b).

In cyanobacteria, Ci uptake is tightly regulated at the transcriptional level. CCM-related genes encoding many components of Ci transporters are maximally expressed under Ci-limiting conditions (i.e. in ambient air [low CO_2 {LC}]) but are repressed at elevated CO_2 levels (high CO_2 [HC]; Wang et al., 2004). Three transcriptional regulators of Ci utilization have been identified in the model cyanobacterium *Synechocystis* sp. PCC 6803 (hereafter, *Synechocystis* 6803): (1) the cyanobacterial homolog of the transition state regulator from *Bacillus subtilis* called cyAbrB2 (*sll0822*), (2) the regulator of the ATP-dependent bicarbonate transport system called CmpR (*sll0030*), and (3) NdhR (also called CcmR, CO_2-concentrating mechanism regulator; *sll1594*). cyAbrB2 regulates the transcription of genes associated with both carbon and nitrogen metabolism (Ishii and Hihara, 2008; Lieman-Hurwitz et al., 2009; Kaniya et al., 2013). The regulator CmpR activates the expression of the *cmpABCD* operon encoding the high-affinity bicarbonate transporter called BCT1, which is induced under LC conditions (Omata et al., 2001). Generally, NdhR, also called CcmR, is regarded as the most important regulator of Ci utilization. NdhR primarily acts as a repressor of the genes encoding components of Ci transporters, such as NDH-1_3 and the sodium-dependent bicarbonate transporter called SbtA, under HC conditions (Figge et al., 2001; Wang et al., 2004; Woodger et al., 2007). Both NdhR and CmpR belong to a large family of LysR-type transcriptional regulators (LTTRs; Schell, 1993) that change DNA-binding properties upon binding to small effector molecules. Recently, the metabolic signals for CmpR and NdhR were identified. The promoter binding of the activator CmpR is stimulated through 2PG and RubP (Nishimura et al., 2008). For the repressor NdhR, the metabolites 2-oxoglutarate (2OG) and $NADP^+$ have been confirmed as corepressor molecules (Daley et al., 2012), thereby increasing the binding of this repressor to two regions upstream of *ndhR* (*sll1594*) and *ndhF3* (*sll1732*; Figge et al., 2001).

Existing transcriptomic data sets for the response of cyanobacteria to LC shifts are restricted to protein-coding genes (Wang et al., 2004; Eisenhut et al., 2007; Schwarz et al., 2011). Although widely accepted as important regulatory elements, small RNAs (sRNAs) were not included in the previous studies. Recent transcriptome analyses revealed a high number of non-protein-coding RNAs (ncRNAs) in *Synechocystis* 6803 (Georg et al., 2009; Mitschke et al., 2011; Kopf et al., 2014a). Several ncRNAs have been identified as important posttranscriptional regulators of photosynthetic gene expression. For example, a Ci-regulated antisense RNA (asRNA), As1_flv4, prevents the premature expression of the flavodiiron protein 2-4, *flv4-2* (*sll0217-19*) operon after a sudden downshift in Ci supply (Eisenhut et al., 2012). In addition to cis-encoded asRNAs, trans-encoded sRNAs also play an important role, such as PHOTOSYNTHESIS REGULATORY RNA1 (PsrR1). Indeed, PsrR1 is up-regulated after high-light treatment or CO_2 depletion and controls the expression of several genes encoding photosynthetic proteins (Georg et al., 2014). The results of a recent study showed that the sRNA CARBON STRESS-INDUCED RNA1 (CsiR1) was highly expressed under most of the tested conditions but repressed upon long-term cultivation in HC (Kopf et al., 2014a).

In addition to transcriptomics, metabolomics has been applied to characterize changes in the pool sizes of cyanobacterial cells under different Ci levels (Schwarz et al., 2013). Isotope tracing studies demonstrated the reorganization of carbon fluxes in *Synechocystis* 6803 cells after shifts from HC to LC (Huege et al., 2011; Young et al., 2011). A metabolic signature characteristic for cells under Ci-limiting conditions has emerged from steady-state metabolic profiles, in which LC-grown cells of *Synechocystis* 6803 show transiently increased levels of photorespiratory intermediates, the long-term accumulation of glycolytic metabolites, and a decrease in nitrogen assimilation, resulting in reduced levels of amino acids, such as Glu, Gln, and Asp (Eisenhut et al., 2008a; Hackenberg et al., 2012; Schwarz et al., 2014).

Here, we present a comprehensive analysis of transcriptomic and metabolic changes upon a shift in Ci supply in wild-type *Synechocystis* 6803 and Δ*ndhR* mutant cells defective in the main Ci regulator, NdhR. We analyzed the structure of NdhR target promoters and describe the corresponding DNA-binding motif comprising an imperfect inverted repeat. The transcriptome data revealed the responses of several ncRNAs to changing Ci availability and specifically verified the Ci-dependent expression of CsiR1, which might belong to an additional NdhR-independent circuit of Ci regulation. Although a typical LC-related transcriptional pattern was observed in Δ*ndhR* under HC conditions, LC-related metabolic changes were not detected. However, this preacclimated status likely led to a less severe metabolic change in the response to shifts from HC to LC. Moreover, this preacclimation is not achieved at the expense of a reduced growth rate in the Δ*ndhR* mutant under HC conditions (Wang et al., 2004; this study). However, growth deficiency of the mutant was observed under LC. Therefore, these data suggest the existence of additional layers of control between transcriptional and metabolic activities in response to changing Ci availability.

RESULTS

Advanced Transcriptomics Revealed New Ci-Regulated Transcripts

Using a custom-made microarray comprising recently identified new open reading frames (norfs) and ncRNAs of *Synechocystis* 6803 (Mitschke et al., 2011), we analyzed the global transcriptomic response to changes in Ci availability (Supplemental Tables S1 and S2). A genome-wide graphical overview of probe localization and signal intensities is shown in Supplemental Data Set S1. An overview of the overlap with the data obtained using previously described array designs (Wang et al., 2004; Eisenhut et al., 2007) is shown in Tables I and II and Supplemental Figure S1. Thus, the results obtained here concerning protein-coding genes are consistent with and extend previous observations. One example is the gene *norf1* (3-fold up-regulated; Supplemental Table S1), encoding a 48-amino acid protein widely conserved in cyanobacteria (Mitschke et al., 2011), which was not included in previous microarray studies.

Moreover, we identified many Ci-regulated asRNAs. In addition to As1_flv4, whose expression is decreased upon LC shift (Eisenhut et al., 2012), significant Ci-related expression changes were detected for 51 additional asRNAs (Table III; Supplemental Table S3). Among these asRNAs, a second *flv4* gene asRNA (As2_flv4) was identified as a potential backup for the As1_flv4-dependent delay in Flv4 protein synthesis (Eisenhut et al., 2012). As2_flv4 showed a pattern similar to As1_flv4, but the expression changes were rather weak (−0.65 after 24 h of LC; Supplemental Table S1). Two additional asRNAs (*sll1732*-as1/-as2), previously implicated in the posttranscriptional regulation of genes for the $NDH1_3$ complex (*sll1732*–*sll1735*; Daley et al., 2012), were not Ci regulated in our data set (Supplemental Table S1). Moreover, we identified nine asRNAs with a more than 2-fold increase after 24 h under LC and a corresponding decrease in the levels of the cognate mRNAs. Two decreased asRNAs and an increase in complementary mRNAs were observed (Table III). This inverse relationship might indicate a regulatory effect of these asRNAs on the cognate mRNAs. This relationship was observed for three different ribosomal proteins and the translation elongation factor G2 (*fusB*; *sll1098*). Moreover, genes encoding several enzymes, such as transketolase, which links the pentose phosphate pathway to glycolysis, uroporphyrinogen decarboxylase, and adenylosuccinate synthetase, as well as the acyl carrier protein, which is involved in fatty acid biosynthesis, could be regulated through cognate asRNAs. We conclude that several of the Ci-regulated asRNAs might contribute to the regulation of selected metabolic routes under LC.

In addition to asRNAs, trans-encoded sRNAs are involved in posttranscriptional regulation. Recently, the sRNA CsiR1 was expressed under most of the tested conditions (analyzed with cells grown at LC) but repressed under HC (Kopf et al., 2014a). Consistently, in the microarray data set obtained herein, CsiR1 was among the most highly induced transcripts (log_2 fold change of 5.7) in cells shifted from HC to LC (Fig. 1A and Table IV). The expression kinetics was further investigated through northern blotting. CsiR1 was detected at 4 h after the shift to LC, with expression levels peaking within 12 to 24 h (Fig. 1B) and remaining at a constant high level, even under long-term LC acclimation. However, upon transfer to HC, CsiR1 was not detected after 24 h (Fig. 1B), suggesting that CsiR1 is repressed at elevated CO_2 levels. To determine whether the observed effects reflect transcriptional or posttranscriptional control, we fused the luciferase reporter genes *luxAB* to the sequence upstream of *csiR1* ranging from −299 to +1 (+1 designates the transcriptional start site [TSS]; data extracted from Mitschke et al., 2011), and the results showed Ci-dependent luciferase expression (Fig. 1C).

Table I. *Comparison of features (mRNAs or ncRNAs) for Synechocystis 6803 that are covered by microarrays used in this study and in previously published studies*

The array design used in this study is based on Mitschke et al. (2011). The design used in previous studies was extracted from Wang et al. (2004) and Eisenhut et al. (2007). –, Not included; UTR, untranslated region.

Features	Literature	This Study
Annotated genes	3,264	3,364
5′ UTRs	–	708
Antisense RNAs	–	1,940
Potential ncRNAs and additional 5′ and 3′ UTRs	–	602

Table II. *Comparison of previously reported expression changes in Synechocystis 6803 upon a sudden downshift in Ci supply with the data of this study*

A transcript was regarded as induced or repressed if the log_2 fold change was greater than 1 ($P < 0.05$). Literature values were extracted from supplemental tables of Wang et al. (2004; 3 + 12 h after Ci downshift) and Eisenhut et al. (2007; 24 h after Ci downshift). For the evaluation, only ncRNAs were considered, which are clearly annotated according to Mitschke et al. (2011). n.i., Not investigated; –, Not included.

Features with Expression Changes after Shifting Cells for Different Times from High CO_2 to Low CO_2			Literature	This Study
		h		
mRNAs	Induced	3	22	95
		12	144	n.i.
		24	221	93
	Repressed	3	7	146
		12	187	n.i.
		24	277	176
asRNAs	Induced	3	–	27
		24	–	40
	Repressed	3	–	14
		24	–	12
Potential ncRNAs	Induced	3	–	11
		24	–	24
	Repressed	3	–	15
		24	–	10

Table III. *Changes in the abundance of asRNAs in wild-type cells of Synechocystis 6803 in response to a sudden shift in Ci supply*

Values are given as $\log_2$ fold changes and were regarded as significant (asterisks) if the $\log_2$ value was −1 or less or 1 or more and the *P* value was 0.05 or less. Inverse regulated and equal regulated asRNA-mRNA pairs are described. The data are sorted by the fold change value of the asRNA at 24 h of LC. NA, Not available.

asRNA			mRNA			Annotation	
asRNA	3 h of LC	24 h of LC	Gene	3 h of LC	24 h of LC	Gene Symbol	Protein Names
Inverse regulated asRNA-mRNA pairs							
sll1804-as1	1.65*	2.23*	*sll1804*	−2.64*	−3.00*	*rpsC (rps3)*	30S ribosomal protein S3
slr0423-as1	2.14*	1.86*	*slr0423*	−1.19*	−1.24*	*rlpA*	RlpA-like protein
sll1098-as1	2.29*	1.70*	*sll1098*	−1.63*	−1.38*	*fusB (fus)*	Elongation factor G2
sll1800-as2	1.48*	1.56*	*sll1800*	−2.24*	−2.75*	*rplD (rpl4)*	50S ribosomal protein L4
slr0536-as1	0.85	1.52*	*slr0536*	−1.32*	−1.25*	*hemE*	Uroporphyrinogen decarboxylase
sll1070-as2	2.02*	1.28*	*sll1070*	−1.48*	−1.22*	*tktA*	Transketolase
sll1823-as1	1.84*	1.10*	*sll1823*	−2.58*	−2.46*	*purA*	Adenylosuccinate synthetase
ssl1426-as1	0.67	1.04*	*ssl1426*	−1.55*	−1.95*	*rpmI (rpl35)*	50S ribosomal protein L35
ssl2084-as1	0.83	1.04*	*ssl2084*	−1.00*	−1.30*	*acpP*	Acyl carrier protein
slr1146-as3	−1.00*	−1.52*	*slr1146*	0.89	1.43*	NA	Hypothetical protein
As1_flv4 (*sll0217*-as2-0-x)	−3.03*	−2.51*	*sll0217*	5.58*	4.95*	*flv4*	Flavodiiron protein Flv4
Equal regulated asRNA-mRNA pairs							
slr1397-as1	0.22	1.16*	*slr1397*	0.19	1.11*		Unknown protein

When the reporter strains were initially grown under LC conditions, bioluminescence was detectable, suggesting P_{CsiR1} activity. However, the promoter activity decreased upon HC shift. The luminescence was decreased 50% after 4.5 h and reached background levels after 24 h under HC. Thus, the dynamics of luciferase expression were consistent with the observed time course of CsiR1 accumulation. We concluded that the CsiR1 promoter P_{CsiR1} is under Ci-dependent transcriptional control. When the sequence downstream of *csiR1* (covering 323 bp upstream of the start codon of *slr1214*) was tested in the reporter gene assays, no bioluminescence was observed, suggesting that the CsiR1 promoter also drives the expression of the downstream gene *slr1214*, for which a strong induction in LC-grown cells has been reported previously (Wang et al., 2004), likely reflecting imperfect termination at the CsiR1 3′ end.

In addition to CsiR1, many other sRNAs were also up- or down-regulated upon Ci downshift, including Non-coding RNA 0700, Ncr0700, and Nitrogen stress-induced RNA4, NsiR4 (Table IV), for which strong expression changes in response to light or nitrogen depletion have been described (Kopf et al., 2014a). Similar to the well-characterized sRNA PsrR1, a post-transcriptional regulator of photosynthesis genes (Georg et al., 2014), the Ci-regulated sRNAs might also be implicated in regulatory processes. However, the potential targets of these sRNAs remain unknown. Next, we examined how the expression of these sRNAs is associated with the Ci regulatory network.

Mutation of *ndhR* Has Only Minor Effects on the Ci-Regulated ncRNAs

Using an optimized microarray platform, we also analyzed the transcriptomic response in the Δ*ndhR* mutant. The entire expression data set of sRNAs, asRNAs, and mRNAs for protein-encoding genes is displayed in Supplemental Table S2. The expression of only some ncRNAs changed in the Δ*ndhR* mutant compared with the wild type, whereas the majority of these RNAs remained Ci regulated. For example, the sRNA CsiR1 was not present under HC and accumulated in LC-shifted Δ*ndhR* cells, suggesting that the expression of CsiR1 is independent of NdhR. However, the induction of CsiR1 was slower after the LC shift compared with the wild type (i.e. the CsiR1 transcript level was less highly induced at 3 h after LC shift in Δ*ndhR* but reached similar levels to the wild type after 24 h of LC; Table IV). This delayed induction was also observed for many other LC-induced, but not NdhR-regulated, genes in the Δ*ndhR* cell background, reflecting the preacclimated state of this mutant (discussed below in more detail). However, the putative sRNA Ncr0210 was NdhR regulated, showing a more than 2-fold increase in Δ*ndhR* under HC (Fig. 2; Table IV). Ncr0210 is transcribed from a region downstream of the protein-coding gene *slr1592*, which is also NdhR regulated (see below). Moreover, the microarray analysis revealed that the expression of asRNA *sll1730*-as1 increased more than 3-fold in Δ*ndhR* compared with the wild type under HC conditions. This asRNA is complementary to regions of *sll1730*, which encodes a protein of unknown function and is not Ci regulated. However, the detailed analysis revealed that this asRNA also overlaps with the TSS of the adjacent gene *sll1732* (*ndhF3*), which is elevated in Δ*ndhR* under HC (Fig. 2).

The *ndhR* Mutation Affects mRNAs Belonging to Different Groups

The data set generated in this study contained many genes that are up-regulated under HC conditions in Δ*ndhR* relative to wild-type cells (Table V; Supplemental Fig. S2), in which these genes are

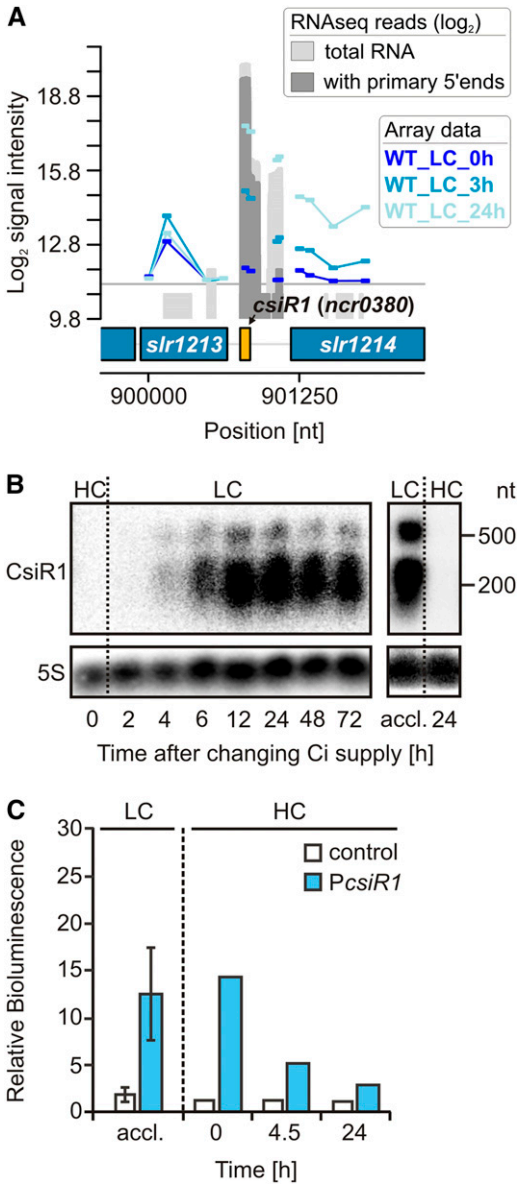

Figure 1. The Ci-regulated ncRNA CsiR1. A, Genomic locus of the ncRNA CsiR1 with mapped array probes. The signal intensities are given as $\log_2$ values. The gray graphs represent RNA sequencing data given as $\log_2$ read numbers, which were extracted from Mitschke et al. (2011). These data indicate that strong induction of CsiR1 probably also drives the expression of the downstream gene *slr1214* (*response regulator 15*, light and stress integrating response regulator, *lsiR*), whose strong induction upon a downshift in Ci supply has been reported earlier (Wang et al., 2004). B, Ci-dependent expression kinetics of CsiR1 analyzed by northern blotting. Cells were precultivated in the presence of HC (5% CO_2), and then CO_2 supply was reduced (LC; 0.040%). Long-term LC-acclimated cells (accl.; 1 week) were again shifted to HC. C, Verification of the CsiR1 Ci-dependent promoter activity using *luxAB* reporter gene fusions whose expression was measured as bioluminescence in vivo. For the promoter analysis, the upstream sequence from −299 to +1 with respect to the *csiR1* TSS (+1) was used. Data for LC are means ± SD obtained with triplicates (independent transformants) in three independent experiments. The shift to HC was performed twice. nt, Nucleotides; WT, wild type.

typically induced under LC according to Wang et al. (2004). These results suggested that NdhR is an HC-dependent repressor. In contrast to previous studies, we also analyzed cells shifted for 3 and 24 h under LC conditions to characterize long-term Ci-dependent transcriptional regulation. Interestingly, we noted additional LC-induced changes in the mRNA levels of many genes, which were deregulated in Δ*ndhR* under HC and therefore not expected to be further affected through changes in the Ci supply. According to the Ci and/or NdhR regulation pattern of transcript accumulation, we defined five categories of genes differently affected through the *ndhR* disruption in cells under HC or LC conditions (Fig. 3).

The genes in category I were fully expressed in the Δ*ndhR* background under HC, and no further increase in transcript abundance was observed after the LC shift. For example, category I contains the putative operon *slr2006-slr2013*, encoding the subunits of a multicomponent Na^+/H^+ antiporter complex. The transcript abundances of category I genes were higher in mutant than in wild-type cells at all three time points under HC and at 3 and 24 h under LC. The genes in category II, such as *sll1732* (*ndhF3*), also showed increased transcript abundance in Δ*ndhR* under HC, but these genes were further stimulated after the LC shift and might be regulated through an additional factor. Category III comprises the genes that were not LC induced in wild-type cells but whose expression was strongly enhanced in Δ*ndhR* under HC compared with wild-type cells. In addition to *sll0529* (annotated as a hypothetical protein with similarities to a phosphoketolase) and *slr1592* (putative pseudouridine synthase), for which an up-regulation in Δ*ndhR* was also reported (Wang et al., 2004), *sll0834*, which encodes the Na^+-bicarbonate symporter BicA, is a new member of the category III genes. Interestingly, the transcript levels of all three genes were decreased in Δ*ndhR* cells after long-term LC, further suggesting the additional regulation of some NdhR-regulated genes. The category IV genes showed strong down-regulation in Δ*ndhR* cells under HC, indicating that NdhR might also function as a transcriptional activator. An example in this category is the gene *slr0907*, which encodes a giant protein containing a GT1 family glycosyltransferase and a methyltransferase domain. In addition to the role of NdhR in LC-stimulated gene expression, we also observed that NdhR might be implicated in the down-regulation of some genes, defined as category V, under LC conditions. For example, *slr1302* (CO_2 uptake protein B, *cupB*) is normally expressed at lower levels under LC conditions but showed no decrease in LC-treated Δ*ndhR* cells. The category V genes might be inversely NdhR regulated (i.e. the expression of these genes is suppressed through NdhR binding under LC). A full list of significant expression changes and gene classifications is provided in Table V.

In addition to the changed expression of the genes in categories I to V, we observed that many of the remaining LC-induced genes, which did not show

Table IV. *Changes in the abundance of potentially trans-encoded ncRNAs in the wild type and the mutant ΔndhR of Synechocystis 6803 in response to a sudden shift in Ci supply*

Values are given as $\log_2$ fold changes and were regarded as significant (asterisks) if the $\log_2$ value was −1 or less or 1 or more and the *P* value was 0.05 or less. For each strain, the expression values at HC were used as reference. Fold changes between the wild type and Δ*ndhR* under HC were calculated by subtracting the corresponding wild-type value. The columns are sorted by the fold change values for the wild type at 24 h of LC. It should be noted that only ncRNAs with an annotation based on Mitschke et al. (2011) were considered here. However, due to the fixed-distance algorithm that was used to classify ncRNAs, there might be some overlap with UTR annotations (e.g. ncl0690 is found upstream of *ndhR* and includes its 5′ UTR).

Systematic Name	Annotation	Wild Type		Δ*ndhR*		Δ*ndhR*-Wild Type at HC
		3 h of LC	24 h of LC	3 h of LC	24 h of LC	
NC-425	CsiR1, SyR14, ncr0380	3.03*	5.69*	0.59	5.64*	0.07
NC-101	ncr1200	1.94*	3.85*	0.80	4.22*	−0.16
NC-392	ncr0840	2.60*	2.71*	1.09	2.82*	0.12
NC-423	ncr0700	1.75*	2.66*	1.38*	2.68*	0.30
NC-55	ncr0240	1.96*	2.65*	1.45*	3.01*	−0.02
NC-137	ncr1350	0.80	2.05*	0.47	1.66*	−0.33
NC-247	ncl0570	0.28	1.94*	0.13	2.02*	−0.13
NC-115	ncr1500	0.23	1.80*	0.23	1.82*	−0.04
NC-97	ncl1110	−0.17	1.68*	−0.21	2.00*	−0.08
NC-248	ncr1240	0.63	1.67*	0.27	1.87*	−0.02
NC-443	SyR52, ncl1790	0.49	1.49*	0.50	1.85*	−0.01
NC-319	ncl0690	1.56*	1.34*	0.15	1.00	3.29*
NC-388	ncr1650	1.04*	1.25*	0.54	1.70*	−0.01
NC-17	ncl0170	0.14	1.24*	0.36	1.19*	−0.72
NC-261	ncr0080	0.78	1.19*	0.40	1.45*	−0.14
NC-372	ncl1060	−0.15	1.19*	−0.05	1.73*	0.03
NC-239	ncr1280	1.79*	1.16*	1.48*	0.30	0.28
NC-430	ncr0210	0.74	1.14*	−0.36	−0.71	1.58*
NC-272	ncr0530	0.35	1.13*	0.19	1.02*	−0.07
NC-168	ncl1350	0.00	1.12*	0.33	0.61	−0.26
NC-237	ncl1700	0.16	1.10*	0.08	1.36*	−0.06
NC-262	ncr1220	−0.09	1.07*	−0.18	1.19*	0.02
NC-404	ncl1010	0.13	1.07*	0.31	0.72	0.01
NC-135	ncl0440	0.75	1.02*	0.23	0.80	0.05
NC-639	ncl0215	−0.71	−1.31*	−0.44	−1.44*	−0.02
NC-22	ncr1020	−1.26*	−1.39*	−1.10*	−1.34*	−0.02
NC-250	ncr1390	−1.56*	−1.51*	−0.88	−1.47*	−0.34
NC-230	ncl0540	−2.02*	−1.52*	−0.75	−1.96*	−0.54
NC-412	ncl0110	−1.42*	−1.55*	−1.19*	−1.55*	−0.04
NC-171	NsiR4, SyR12, ncl0540	−2.22*	−1.58*	−0.81	−1.97*	−0.58
NC-318	ncl1500	−1.83*	−1.66*	−0.53	−2.20*	−0.19
NC-334	ncl1330	−1.80*	−1.84*	−0.08	−1.97*	−0.41
NC-146	ncl0380	−1.85*	−1.90*	−1.17*	−1.86*	−0.12
NC-240	ncr1660	−2.61*	−3.18*	−1.92*	−3.36*	−0.10

changes in the mutant Δ*ndhR* (e.g. *flv4* or *cmpA*), showed a delayed response after LC shift (i.e. the mRNA levels were typically lower after 3 h under LC in Δ*ndhR* compared with the wild type, but equal levels were observed after 24 h; Supplemental Table S4). This slower response was also observed for several LC-induced ncRNAs, and this effect is consistent with the derepression of many genes encoding CCM components in the Δ*ndhR* mutant strain under HC, leading to the preacclimation of mutant cells to LC conditions.

Definition of the NdhR-Binding Motif

NdhR belongs to the LTTR family that commonly bind to palindromic DNA sequences forming an imperfect dyadic region (Schell, 1993; Maddocks and Oyston, 2008). Moreover, LTTR proteins are frequently autoregulatory (i.e. these proteins bind and regulate their own promoters). Correspondingly, we observed a 3-fold increase of the *ndhR* mRNA levels after the shift from HC to LC in wild-type cells (Supplemental Table S1), likely reflecting the release of NdhR from the promoter, consistent with Figge et al. (2001). The consensus binding motif of all LTTRs was defined as T-N_{11}-A (Goethals et al., 1992), which is also part of the previously reported putative NdhR motif (TCAATG-N_{10}-ATCAA; Figge et al., 2001). However, this motif is not present in the upstream regions of the deregulated genes in Δ*ndhR*. Hence, we speculated that NdhR might bind to a different DNA sequence. Making use of the currently available comprehensive genomic

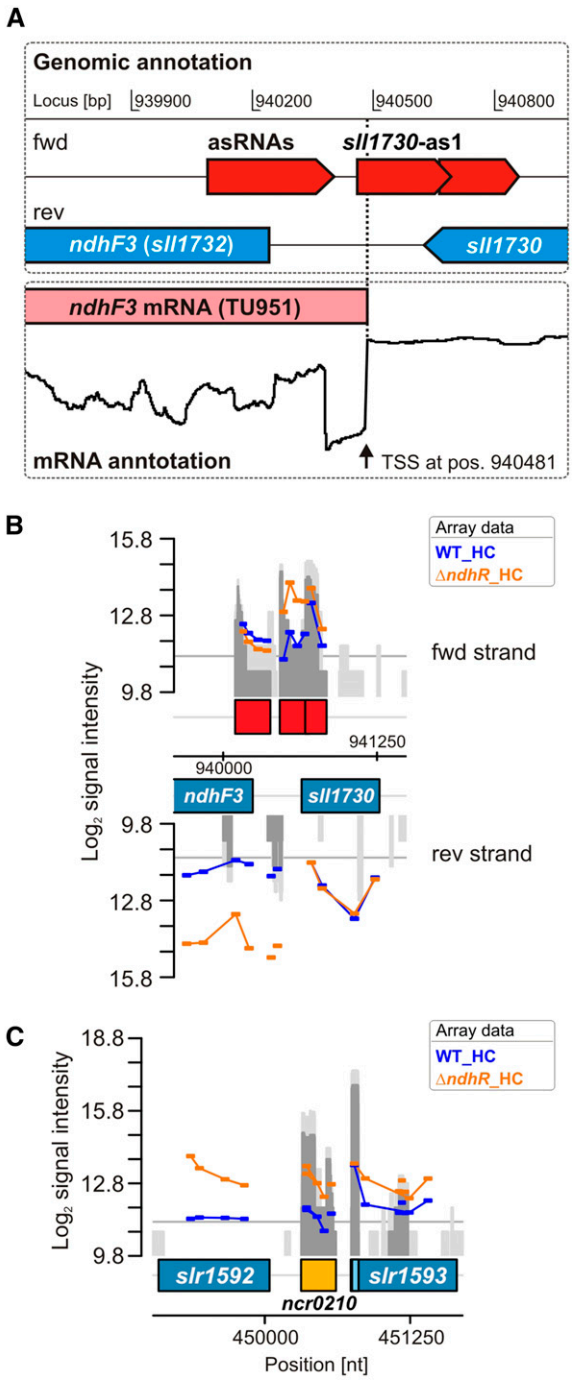

Figure 2. Identification of NdhR-regulated asRNAs and potentially trans-encoded ncRNAs. A, Transcriptional organization of the *ndhF3* gene, for which an increased transcript accumulation was observed in Δ*ndhR*. The localization of asRNAs was extracted from Mitschke et al. (2011). Differential RNA sequencing (Kopf et al., 2014a) revealed the TSS of the *ndhF3* gene. Interestingly, one asRNA (*sll1730*-as1), which was originally mapped to *sll1730*, because it overlaps its coding region, also overlaps with 21 nucleotides of the 5′ end of the *ndhF3* mRNA (TU951). B, Array signals for probes covering the same genomic region. Transcription of this asRNA also appeared higher in Δ*ndhR*. C, Array signals for a putatively NdhR-regulated ncRNA, Ncr0210, which is localized downstream of *slr1592* and also appeared to be NdhR regulated (compare with Table V, class III genes). nt, Nucleotides; WT, wild type.

information, we conducted a comparative analysis of *ndhR* promoters among cyanobacteria, assuming the autoregulation of this promoter, as in *Synechocystis* 6803. A 300-bp sequence upstream of the *ndhR* start codon was extracted from strains closely related to *Synechocystis* 6803, such as *Synechococcus* sp. PCC 7002, *Cyanothece* sp. ATCC 51142, *Pleurocapsa* sp. PCC 7327, and *Microcystis aeruginosa* PCC 9717, to identify conserved promoter motifs. In addition to *ndhR*, NdhR binding was verified for the promoter of the bicarbonate transporter gene *bicA* in *Synechococcus* sp. PCC 7002 (Woodger et al., 2007). Interestingly, in *Synechococcus* sp. PCC 7002, *bicA* is clustered with genes similar to *slr2006-2013*, which are also NdhR regulated in *Synechocystis* 6803. Hence, sequences upstream of *bicA* were also extracted from cyanobacterial genomes, showing a similar *bicA* organization to that in *Synechococcus* sp. PCC 7002. The extracted sequences were analyzed using the MEME search tool (Bailey et al., 2009), and the results revealed the common motif ATNGN$_7$TCTAT. This sequence was also identified upstream of many genes, including *sbtA*, *ndhF3*, and *slr2006*, showing changed expression in *Synechocystis* 6803 Δ*ndhR* mutant cells (Fig. 4A). The same motif was also observed upstream of *bicA*, although this gene was not LC induced in *Synechocystis* 6803 to the same extent as in *Synechococcus* sp. PCC 7002. However, according to the data obtained in this study, *bicA* is apparently NdhR regulated in *Synechocystis* 6803, as the mRNA level of this gene was increased in Δ*ndhR* (Table V). The ATNGN$_7$TCTAT motif is located downstream of the -10 element and the TSS in NdhR-regulated promoters of *Synechocystis* 6803. These sites were used to refine the consensus sequence, namely ATAG-N$_8$-CTAT (Fig. 4B). Interestingly, the NdhR-binding motif is also observed upstream of *bicA* in *Synechococcus* sp. PCC 7002. The role of NdhR binding for *bicA* expression perfectly corresponds to the data obtained from previous studies involving promoter test experiments using a reporter gene approach, showing the derepression of truncated *bicA* promoters that miss the NdhR-binding motif identified herein (Fig. 4C; data extracted from Woodger et al., 2007). Moreover, this consensus motif is present twice upstream of the *ndhR* gene in *Synechocystis* 6803. Previous studies have shown that only promoter fragments harboring these motifs displayed in vitro NdhR binding, whereas promoter versions without the motif did not bind NdhR (Fig. 4D; data extracted from Figge et al., 2001).

The Metabolic Response of the Δ*ndhR* Mutant to the LC Shift

The transcriptome data revealed that many genes specifically induced in the wild type through a shift from HC to LC were also expressed at increased levels in the Δ*ndhR* mutant under HC. These observations are consistent with a function of NdhR as a major transcriptional regulator that adjusts the physiological status of *Synechocystis* 6803 to the changing Ci supply.

Table V. *Genes whose expression was affected by ndhR mutation in Synechocystis 6803*

Values are given as $\log_2$ fold changes and were regarded as significant (asterisks) if the $\log_2$ value was −1 or less or 1 or more and the *P* value was 0.05 or less. Fold changes between the wild type and Δ*ndhR* were calculated for each time point by subtracting the corresponding wild-type value. Categories were defined based on the regulatory pattern observed after Ci downshift (for explanations, see text). For comparison reasons, the $\log_2$ fold changes of Δ*ndhR* observed by Wang et al. (2004; only HC conditions were considered there [n.c. = no change]) were compared with the changes observed in this study. The transcriptional organization (operon structure and presence of TSSs) was extracted from Kopf et al. (2014a). NA, Not available.

Identifier	Gene Name	Protein Name	Wang et al. (2004) at HC	Δ*ndhR*-Wild Type			Category Type	Operon	First Gene of Cluster	Motif Upstream
				HC	3 h of LC	24 h of LC				
slr2006	NA	Hypothetical protein	5.84	4.30*	3.19*	3.32*	I	a	+	+
slr2007	*ndhD5*	NADH dehydrogenase subunit 4	4.42	3.29*	2.34*	2.58*	I	a	−	−
slr2008	NA	Hypothetical protein	3.20	2.71*	1.57*	1.76*	I	b	+	−
slr2009	*ndhD6*	NADH dehydrogenase subunit 4	2.42	2.21*	1.21*	1.32*	I	b	−	−
slr2010	NA	Hypothetical protein	3.16	2.34*	1.27*	1.36*	I	b	−	−
slr2011	NA	Hypothetical protein	2.19	2.21*	1.10*	1.29*	I	b	−	−
slr2012	NA	Hypothetical protein	1.80	2.22*	1.11*	1.38*	I	b	−	−
slr2013	NA	Hypothetical protein	1.69	1.74*	0.69	0.86	I	b	−	−
ssr3409	NA	Hypothetical protein	1.61	2.41*	1.31*	1.53*	I	b	−	−
ssr3410	NA	Hypothetical protein	3.15	2.50*	1.47*	1.59*	I	b	−	−
sll1732	*ndhF3*	NADH dehydrogenase subunit 5 (involved in low CO_2-inducible, high-affinity CO_2 uptake)	4.22	2.78*	−0.92	0.90	II	c	+	+
sll1733	*ndhD3*	NADH dehydrogenase subunit 4 (involved in low CO_2-inducible, high-affinity CO_2 uptake)	4.25	2.63*	−0.86	0.94	II	c	−	−
sll1734	*cupA*	Protein involved in low CO_2-inducible, high-affinity CO_2 uptake	3.88	2.28*	−0.87	0.91	II	c	−	−
sll1735	NA	Hypothetical protein	2.47	1.77*	−0.75	1.01*	II	c	−	−
slr1512	*sbtA*	Sodium-dependent bicarbonate transporter	3.31	1.76*	−0.95	1.55*	II	d	+	+
slr1513	NA	Periplasmic protein, function unknown	1.43	1.15	−0.77	1.55*	II	d	−	−
sll0529	NA	Hypothetical protein	1.66	1.01*	0.94	0.57	III	No	+	+
sll0834	*bicA*	Low-affinity bicarbonate transporter	n.c.	2.85*	2.55*	1.04*	III	No	+	+
slr1592	NA	Probable pseudouridine synthase	2.10	1.98*	1.62*	1.23*	III	No	+	+
slr0907	NA	Unknown protein	n.c.	−1.24*	−1.73*	−1.04*	IV	e	+	−
sll1862	NA	Unknown protein	n.c.	−0.89	−0.78	−1.02*	IV	No	+	In coding sequence
slr1259	NA	Hypothetical protein	n.c.	−0.20	1.39*	1.87*	V	f	+	−
slr1261	NA	Hypothetical protein	n.c.	−0.18	0.96	1.29*	V	f	−	−
slr1260	NA	Hypothetical protein	n.c.	−0.13	0.81	1.22*	V	f	−	−
slr1302	*cupB*	Protein involved in constitutive low-affinity CO_2 uptake	n.c.	0.07	0.93	1.13*	V	No	+	In coding sequence
slr1535	NA	Hypothetical protein	1.20	0.15	1.47*	0.99	V	No	+	+
ssl3769	NA	Unknown protein	n.c.	−0.02	0.40	1.52*	V	No	+	+

Specifically, we speculated that the Δ*ndhR* mutant might be constitutively preacclimated to a low Ci supply, because these cells lack the regulation of *ndhR* target genes. To examine this hypothesis at the metabolic level, we compared the phenotype of the mutant with that of the wild type under varying Ci supplies using a metabolite profiling platform enriched for the intermediates of central carbon metabolism (Eisenhut et al., 2008a; Schwarz et al., 2011, 2014). The resulting profiles comprised more than 600 mass features for nontargeted metabolome analysis, facilitating the examination of 45 identified metabolites and 18 repeatedly observed, but yet unidentified, analytes (Supplemental Table S5).

We expected that cells preacclimated to low Ci supply should not show the metabolic effects of LC under HC conditions. Consistent with this expectation, Δ*ndhR* mutant and wild-type cells did not show marked metabolic differences under HC conditions, as indicated by the nontargeted independent component analysis (ICA; Fig. 5A) and the supporting significance analysis (Supplemental Table S5). Particularly, we observed no changes in metabolites, such as the photorespiratory metabolites 2PG or glycolate, characteristic of the LC-shift response of wild-type cells under HC conditions (Fig. 6). These compounds were accumulated under HC conditions in the *ccmM* mutant of *Synechocystis* 6803 (Hackenberg et al., 2012). Among

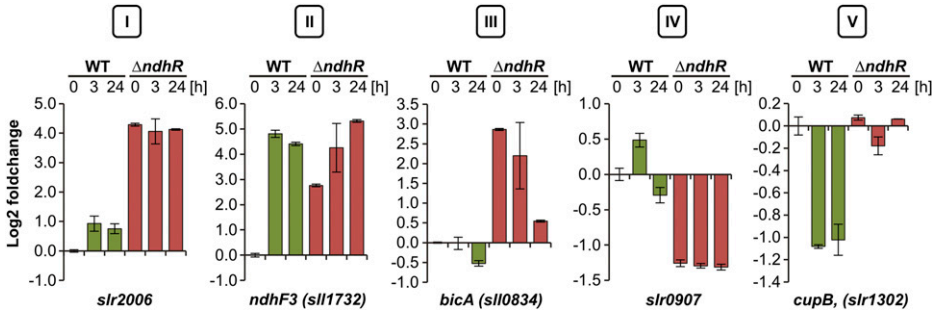

Figure 3. Classification of Ci-regulated protein-coding genes in *Synechocystis* 6803. Different categories of expression patterns were observed in Δ*ndhR* upon sudden downshift in Ci availability: category I, entirely deregulated; category II, derepressed but further induced upon Ci downshift; category III, derepressed in Δ*ndhR* but not inducible by Ci depletion in wild type (WT); category IV, repressed compared with the wild type; and category V, not repressed by Ci depletion as in the wild type. Values are given as $\log_2$ fold changes compared with the wild type grown at HC (0 h).

the few differences between the Δ*ndhR* mutant and wild-type cells under HC conditions was a significant decrease in Glc-6-P, indicating a decrease in soluble sugar metabolism (Fig. 6).

However, consistent with the assumed pre-acclimation under HC conditions in response to low Ci supply, the LC-shifted Δ*ndhR* cells exhibited clear metabolic differences. Nontargeted ICA revealed a delay in metabolic responses to an LC shift in the mutant (Fig. 5A). Specifically, the transient metabolic state of wild-type cells at 3 h was not apparent in LC-shifted mutant cells after either 3 or 24 h. For a more detailed analysis, we classified the metabolites into seven response categories according to changes in the Ci shift-associated relative pool sizes in wild-type cells. Categories IA to IC comprise metabolites with early and maintained, late, or transient increases, respectively, whereas categories IIA to IIC represent the respective inverse behavior, and category III comprises nonresponding metabolites (Fig. 5B; Supplemental Table S5). The early and maintained increases and the transient increases in the metabolites of categories IA and IC were absent in the mutant, delayed, or diminished (Fig. 5B). In contrast, categories IIA to IIC, containing metabolites with generally decreased pool sizes, were largely similar in mutant and wild-type cells. Category IC, with transiently increased metabolites in the wild type but with delayed or unchanged responses in the mutant, contained the photorespiration intermediates 2PG, glycolate, and Gly. Thus, the metabolic behavior of wild-type cells in response to a sudden shift to low Ci supply is referred to as the photorespiratory burst (Fig. 6). The photorespiratory burst did not extend into the Ser, 3-phosphoglycerate, and 2-phosphoglycerate pools. Long-term, LC-induced Ser accumulation, however, was absent in the mutant. The photorespiratory burst was accompanied by the transient accumulation of specific amino acids, namely Thr, Ile, and the joined Arg, Orn, and citrulline pools (Fig. 6). Similar to Ser, Lys and Tyr were early and maintained in wild-type cells but were delayed or absent in the mutant.

Although the Δ*ndhR* mutant and wild-type cells adopted matching metabolic phenotypes at 24 h after the shift to low Ci supply (Figs. 5 and 6), the mutant unexpectedly showed a clear growth deficiency under LC conditions, whereas growth was not significantly affected under HC (Supplemental Fig. S3). The associated significant metabolic differences between the Δ*ndhR* mutant and wild-type cells after long-term LC acclimation were decreased levels of malate, Suc, and glycerol-3-phosphate accompanied by increased levels of glycerol and Ser (Fig. 6; Supplemental Table S5). Thus, here, we conducted an integrated analysis of the metabolic responses and expression of genes encoding the enzymes of photorespiration and central metabolism, revealing that gene expression and the respective metabolic changes in response to low Ci supply were largely unchanged in the Δ*ndhR* mutant (for a graphical overview, see Supplemental Data Set S2).

DISCUSSION

Carbon-Regulated Genes and sRNAs

The switch from HC to LC conditions initiates cellular reprogramming involving the enhanced expression of CCM components, particularly genes for high-affinity Ci transporters. This coordinated up-regulation of specialized transporters, such as BCT1, SbtA, or $NDH1_3$, has previously been demonstrated for many cyanobacterial strains (Omata et al., 1999; Shibata et al., 2001; Woodger et al., 2007). However, transcriptomics using microarrays for *Synechocystis* 6803 (Wang et al., 2004; Eisenhut et al., 2007) revealed that many more genes become activated in LC-shifted cells, indicating that higher CCM activity is not sufficient to fully compensate for the lower external Ci availability. Among these genes, the operon encoding the flavodiiron proteins Flv2 and Flv4 is up-regulated. These proteins play an important role in the protection of PSII under photooxidative stress (Zhang et al., 2012). In addition, we observed increased mRNA levels of the *slr0373-0376*

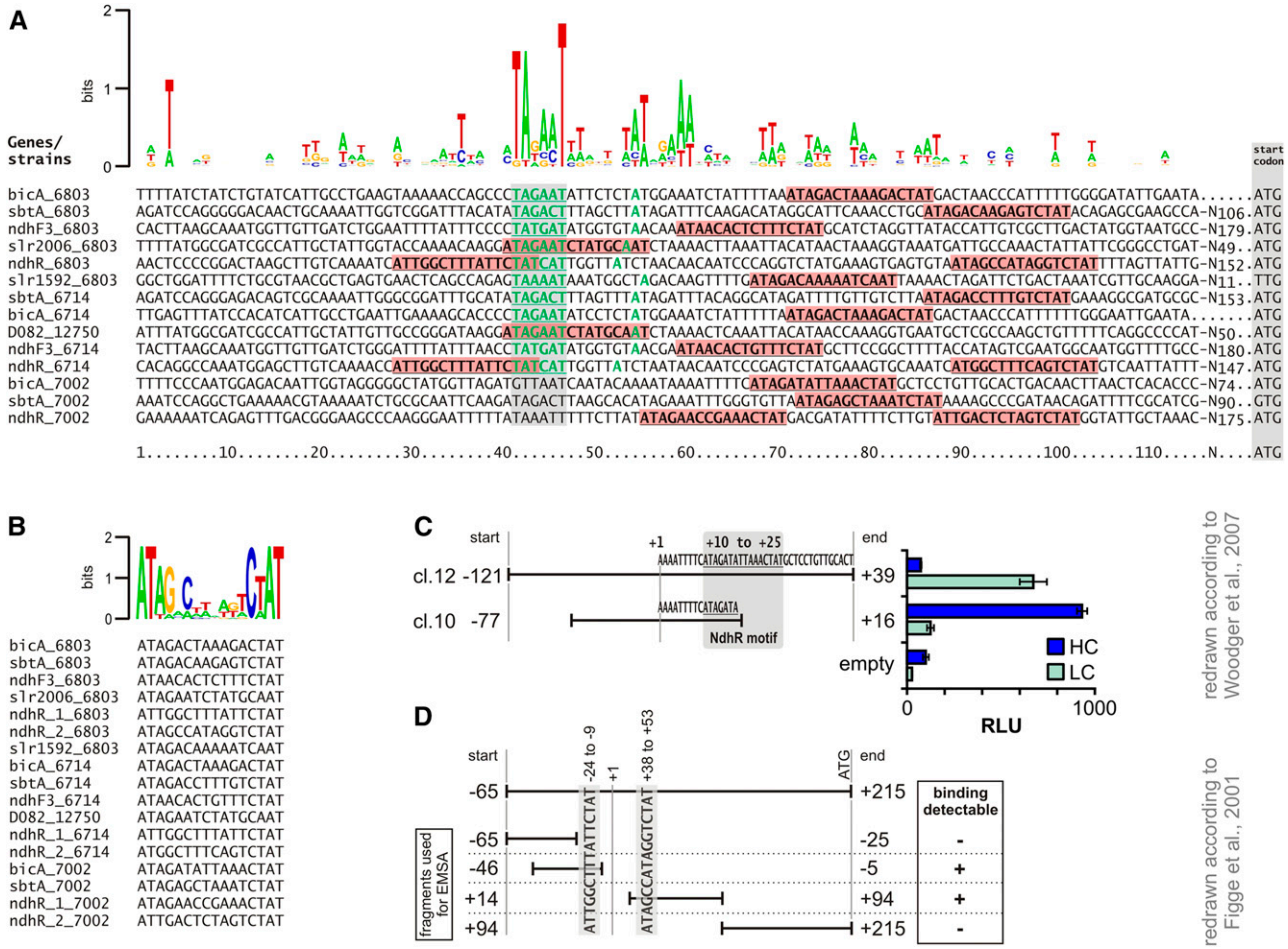

Figure 4. Definition of the NdhR-binding motif using comparative genomics and existing literature data. A, Promoters of NdhR-regulated genes. Initially, a conserved motif was found by comparison of the upstream sequences of the *ndhR* genes from *Synechocystis* 6803, *Synechococcus* sp. PCC 7002, *Cyanothece* sp. ATCC 51142, *Pleurocapsa* sp. PCC 7327, and *M. aeruginosa* sp. PCC 9717 (see text). This was also found upstream of other NdhR-regulated genes in *Synechocystis* 6803 and homologs from *Synechocystis* sp. PCC 6714 or *Synechococcus* sp. PCC 7002 (shown here). The motif (marked by red boxes) is located close to the basal promoter and TSS. Information about the TSS and -10 elements (green letters) was extracted from Mitschke et al. (2011), Kopf et al. (2014a; 6803), and Kopf et al. (2015; 6714). D082_12750 refers to the *slr2006* ortholog in the genome of *Synechocystis* sp. PCC 6714 (Kopf et al., 2014b). B, Alignment of the motifs found upstream of NdhR-regulated genes in *Synechocystis* 6803 and *Synechocystis* sp. PCC 6714 as well as *Synechococcus* sp. PCC 7002, and definition of a consensus motif as ATAG-N_8-CTAT. The sequence comparisons were made manually after detection of the described motif using the MEME search tool. The logos in A and B were generated using the Web server http://weblogo.berkeley.edu. C, In vivo luminescence measurements using strains of *Synechococcus* sp. PCC 7002 carrying two different parts of the *bicA* promoter fused with luciferase genes (data were extracted from Woodger et al., 2007). The gray box marks the position of the identified NdhR motif relative to the analyzed fragments. The full-length promoter of *bicA* repressed luciferase expression at HC but induced it at LC (see cl.12). The truncated promoter used to generate strain cl.10 missed the identified NdhR binding site. The relative luminescence (relative luminescence units [RLU]) of cl.10 at HC was already as high as that observed for cl.12 at LC. It was not further up-regulated, as observed for all other reporter strains (Woodger et al., 2007). D, Summary of electrophoretic mobility shift assay (EMSA) data using the upstream sequence of the *ndhR* gene of *Synechocystis* 6803 (data were extracted from Figge et al., 2001). Two fragments used for EMSA (−65 to +14 and +14 to +94) showed NdhR binding, indicating that at least two NdhR-binding sites exist. The motif identified here is present at positions −24 to −9 and +38 to +53, which are only located within the two fragments bound to NdhR in the EMSA experiments (Figge et al., 2001).

gene cluster, which is transcribed at elevated levels under many stress conditions, including iron starvation (Singh and Sherman, 2002), and encodes proteins of unknown function and the Slr0006 protein, which has homologs in higher plants and might act as a regulatory protein by binding RNA (Carmel et al., 2013). Among the down-regulated genes (Supplemental Table S1), the genes encoding ribosomal proteins and components of nitrogen assimilation, such as *glnA* (*slr1756*), *nrtABCD* (*sll1450-53*), or *amt1* (*ammonium transporter1*; *sll0108*),

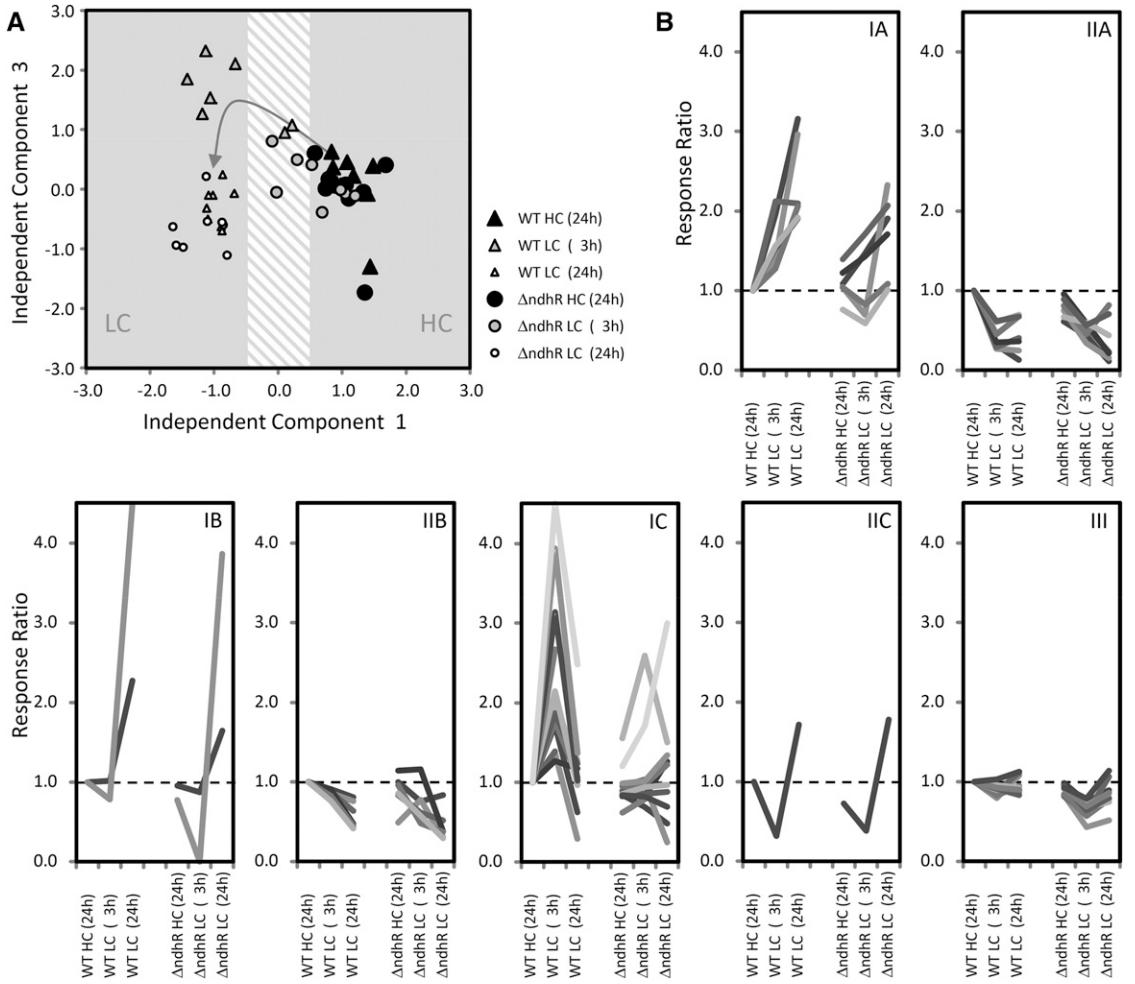

Figure 5. Global analysis of the metabolic responses to a shift from HC to LC conditions in the *Synechocystis* 6803 wild type (WT) compared with the Δ*ndhR* mutant. A, Nontargeted ICA of all observed mass features from gas chromatography-electron ionization-time of flight-mass spectrometry-based metabolite profiles. The transition of the wild-type metabolome (triangles) from HC to LC (described by IC1) via transient changes at 3 h of LC (described by IC3) is indicated by the arrow. The metabolome of the Δ*ndhR* mutant (circles) responds with a delay and does not form the wild-type pattern of transient changes 3 h after the shift to LC. The ICA was based on the first five components of a principal component analysis that covered 46.4% of the total variance of the data set. The data set consists of three independently repeated biological experiments with two to three replicate samples from each culture and condition. B, Classification of the annotated metabolites from our metabolome data set according to their response type in the *Synechocystis* 6803 wild type. Categories IA to IC comprise metabolites with early and maintained (IA), late (IB), or only transient (IC) increases. Categories IIA to IIC represent the respective inverse behavior. Category III contains nonresponding metabolites in the wild type that are significantly changed in the Δ*ndhR* mutant in at least one of the conditions ($P < 0.05$). Categories are based on hierarchical cluster analysis (HCA) using Euclidian distance and complete linkage.

were predominantly identified. The reduced expression is correlated with much lower growth and the relatively increased nitrogen availability of LC-shifted *Synechocystis* 6803 cells. Remarkably, there were few changes in the expression of enzymes participating in the primary carbon metabolism of *Synechocystis* 6803, whereas these genes were often LC regulated in *Synechococcus elongatus* PCC 7942 (Schwarz et al., 2011).

While our expression data on protein-coding genes are consistent with the findings of previous studies, here, we provide, to our knowledge, the first analysis of the impact of varying Ci levels on ncRNAs. Several LC-stimulated asRNAs (Table II) were detected. The asRNAs frequently act as negative regulators of cognate mRNAs, as the binding of the asRNAs leads to codegradation or interferes with translation (Georg and Hess, 2011). Consistent with a codegradation mechanism, we identified 11 mRNA-asRNA pairs with inverse regulation (Table III). Many of these pairs affected the genes for translational machinery, consistent with the down-regulation of translational activity and slower growth under LC. However, some metabolic enzymes were also identified as targets. Thus, in addition to classical protein regulators, such as NdhR,

Metabolite	Response Category	Description of Category	Response Ratios (Averages) WT_24h HC*	WT_3h LC	WT_24h LC	ΔndhR_24h HC	ΔndhR_3h LC	ΔndhR_24h LC	Significance (P<0.05)
Photorespiration									
2PG	IC	increasing (transient)	1	4.8	2.5	1.2	1.7	3.0	LC (3h)
Glycolate	IC	increasing (transient)	1	2.1	1.0	0.9	0.9	1.0	
Glycine	IC	increasing (transient)	1	3.1	1.0	0.8	0.8	0.7	x
Serine	IA	increasing (early maintained)	1	1.3	2.1	1.0	0.8	1.1	x
PGA, PEP Metabolism									
3PGA	III	non-responding	1	0.9	1.2	0.9	1.0	0.9	
2PGA	IA	increasing (early maintained)	1	1.5	1.9	1.2	1.4	1.7	
PEP	IA	increasing (early maintained)	1	2.1	2.1	1.4	1.7	2.1	
Major CHO Metabolism									
Gluconate-6-P	IIA	decreasing (early maintained)	1	0.3	0.1	0.6	0.4	0.1	
Glucose-6-P	IIA	decreasing (early maintained)	1	0.3	0.2	0.7	0.3	0.2	HC (24h)
Fructose-6-P	IIA	decreasing (early maintained)	1	0.4	0.7	0.8	0.5	0.8	
Glucose	IIA	decreasing (early maintained)	1	0.6	0.7	0.9	0.6	0.7	
Sucrose	IIB	decreasing (late)	1	0.9	0.8	0.5	0.8	0.3	x
TCA, Asp, Glu, Gln Metabolism									
Aspartate	IIA	decreasing (early maintained)	1	0.3	0.4	1.0	0.6	0.2	
Malate	III	non-responding	1	0.8	1.1	0.8	0.4	0.5	x
Isocitrate (Citrate)	IIB	decreasing (late)	1	0.9	0.6	0.8	0.6	0.5	x
2OG	IIB	decreasing (late)	1	0.9	0.5	1.1	1.2	0.4	
Glutamate	IIB	decreasing (late)	1	0.8	0.4	1.0	0.5	0.4	
Glutamine (Pyroglutamate, Glutamate)	IIB	decreasing (late)	1	0.8	0.4	0.9	0.6	0.3	x
AA Metabolism									
Threonine	IC	increasing (transient)	1	3.9	1.4	1.0	1.0	1.3	x
Isoleucine	IC	increasing (transient)	1	1.9	1.2	0.9	0.9	0.9	x
Tyrosine	IA	increasing (early maintained)	1	1.6	1.9	0.8	0.6	1.0	x
Lysine	IA	increasing (early maintained)	1	1.4	3.0	1.0	0.7	2.3	LC (3h)
Ornithine (Arginine, Citrulline)	IC	increasing (transient)	1	1.7	0.6	0.8	0.7	0.5	x
Arginine	IC	increasing (transient)	1	2.7	n. d.	0.6	0.8	n. d.	LC (3h)

Figure 6. Overview of Ci-responsive metabolites in the *Synechocystis* 6803 wild type (WT) compared with the Δ*ndhR* mutant. The heat map shows response ratios relative to the wild type at 24 h of HC (asterisk). Metabolites are sorted according to general metabolic context and classified by response category in the wild type (compare with Fig. 5). The significant general difference between the wild type and mutant was assessed by two-way ANOVA (x). Condition-specific differences were tested by heteroscedastic Student's *t* test in LC (3 h) and HC (24 h). For the underlying statistical assessments and the full set of profiled metabolites, see Supplemental Table S5.

asRNA-mediated effects contribute to cellular acclimation in response to LC. Such a mechanism is e.g. responsible for a delay in the LC-stimulated increase in the mRNA levels for the flavodiiron protein Flv4 (Eisenhut et al., 2012). However, asRNAs have also been implicated in transcriptional regulation through NdhR, because asRNAs overlapping the coding region of the NdhR-regulated gene *ndhF3* (*sll1732*) have been detected previously (Mitschke et al., 2011). The potential role for asRNAs as regulatory factors has been proposed previously (Daley et al., 2012), but the asRNAs examined herein were clearly not Ci regulated. An additional asRNA (*sll1730*-as1), originally mapped to the adjacent gene *sll1730*, was also shown to overlap with the 5′ end of the *ndhF3* mRNA (Fig. 2). The expression level of this asRNA was not Ci regulated in wild-type cells but, similar to *ndhF3*, was clearly increased in Δ*ndhR* under HC. Hence, this asRNA might be involved in the posttranscriptional regulation of *ndhF3* though a 21-nucleotide overlap with the mRNA 5′ end. Examples of positively acting asRNAs covering only a part of the 5′ UTR have been reported for *Synechocystis* 6803 (Sakurai et al., 2012).

Moreover, we also observed several LC-regulated ncRNAs. Among them, CsiR1 was specifically induced after LC shift and was suppressed after transfer to HC (Fig. 1). Interestingly, CsiR1 is transcribed from a region upstream of *slr1214*. This gene lacks its own promoter, and expression is driven by read through from CsiR1. The gene *slr1214* encodes an LC-induced two-component response regulator and has been proposed as a candidate for the regulation of the early response to Ci limitation (Wang et al., 2004). However, this assumption is rather unlikely. Recently, it was shown that the Slr1214 response regulator is involved in phototaxis (Narikawa et al., 2011) and UV-A signaling (Song et al., 2011). In addition to CsiR1, many other sRNAs were also up-regulated upon Ci downshift (e.g. Ncr0700, which is induced through low-light intensities or darkness; Kopf et al., 2014a). In contrast, NsiR4, which is induced under nitrogen limitation (Kopf et al., 2014a), was down-regulated under LC. Similar results were also observed for other nitrogen-regulated genes, likely reflecting changes in the carbon-nitrogen ratio.

It is tempting to speculate that the Ci-regulated changes in the mRNA levels are at least partially mediated via asRNAs or sRNAs. Thus, these ncRNAs introduce an additional level of regulation in LC-shifted cells. With the exception of As1_flv4, which is

regulated through cyAbrB (Eisenhut et al., 2012), the transcriptional regulation of sRNAs remains ambiguous. Therefore, we investigated if some of these molecules might also be part of the NdhR regulon, which includes many genes associated with CCM.

Identification of True NdhR Targets through Microarray and Promoter Analyses

To determine whether the regulation via ncRNAs depends on or involves classical regulation through transcription factors, we analyzed the LC response of the mutant Δ*ndhR*, which is defective in the main repressor for LC-regulated genes. Similar to the data of Wang et al. (2004), we observed the up-regulation of 19 protein-coding genes under HC conditions in Δ*ndhR* cells, and the expression of these genes was only induced in wild-type cells after LC shift (Table V). However, only one sRNA (Ncr0210), showing changes in the expression levels under different Ci regimes, was deregulated in Δ*ndhR* cells under HC (Table IV). These data reveal that NdhR primarily acts as a repressor of many LC-induced genes encoding Ci transporters, whereas Ci regulation via ncRNAs is primarily NdhR independent, representing a new and additional mechanism.

Daley et al. (2012) showed that the NdhR repressor is released from the cognate promoters in the absence of 2OG, which was detected at lower levels in wild-type cells at 24 h after the LC shift. A similar decrease in 2OG was measured in a recent comparative analysis of the PII mutant and wild-type cells (Schwarz et al., 2014). However, the kinetics of changes in the relative levels of 2OG and mRNAs of NdhR-regulated genes are different. For example, *sbtA* gene expression peaked at 3 h after the LC shift (Wang et al., 2004), whereas the 2OG level was almost similar to that of HC cells (Fig. 6). It is likely that we missed rapid 2OG changes potentially occurring immediately after the LC shift or changes in the second corepressor molecule, $NADP^+$ (Daley et al., 2012), which are much faster and responsible for the quick release of NdhR from cognate promoters.

Theoretically, the deregulation of a gene in a microarray data set could reflect direct or indirect effects (i.e. the promoter binding of NdhR or the influence of another regulatory mechanism affected by the absence of NdhR). To distinguish between these possibilities, we reconsidered the promoter-binding motif of NdhR. Global transcriptomics using differential RNA sequencing with *Synechocystis* 6803 revealed a comprehensive map of TSSs (Mitschke et al., 2011; Kopf et al., 2014a). These data were used to elucidate whether neighboring NdhR-regulated genes were part of an operon. Indeed, many NdhR-regulated genes are transcribed as part of an operon, reducing the number of true NdhR-targeted promoters (Table V). We selected the upstream regions of NdhR-regulated genes, such as *ndhR*, *sbtA*, *ndhF3*, *slr2006*, and *bicA*, from *Synechocystis* 6803 and from related cyanobacteria that have similar gene organization. The promoter analysis revealed a conserved NdhR-binding motif: ATAG-N_8-CTAT (Fig. 4). Correspondingly, this motif was only detected upstream of the first genes of NdhR-regulated operons. Fortunately, the subfragments of promoters from NdhR-regulated genes involved in NdhR binding (Figge et al., 2001) or mediating the Ci-dependent regulation of reporter genes (Woodger et al., 2007) have been identified previously. These data, generated via experimental promoter analyses, are consistent with the NdhR-binding motif predicted here, as only promoter fragments containing the predicted motif showed NdhR-binding or NdhR-mediated regulation, whereas all fragments lacking this motif were deregulated (Figge et al., 2001; Woodger et al., 2007). However, the correct function of this regulation depends on the motif position relative to the promoter or even additional sequence elements. For example, although the promoter of *bicA* (*sll0834*) contained the described motif, this gene was obviously not Ci regulated in wild-type *Synechocystis* 6803. In contrast, *bicA* expression was strongly elevated in Δ*ndhR* under HC (Fig. 3 and Table V). However, *bicA* is LC induced and NdhR regulated in *Synechococcus* sp. PCC 7002 (Woodger et al., 2007). It is tempting to speculate that the missing LC inducibility of *bicA* in wild-type *Synechocystis* 6803 might reflect a posttranscriptional mechanism, such as sRNA-mediated degradation. The existence of an additional sequence element for correct NdhR function is further supported by evidence that the NdhR-binding sequence also occurs upstream of genes that are not affected through the *ndhR* disruption. These genes include *fbpI* (*slr2094*), which encodes Fru-1,6-sedoheptulose-1,7-bisphosphatase, and *hik9* (*slr0210*), which encodes a sensor His kinase.

Moreover, the data set revealed additional unexpected findings. For example, the gene cluster *slr2006-slr2013*, whose expression is obviously completely deregulated in Δ*ndhR*, was assumed to undergo polycistronic transcription, because all genes were expressed at equal levels and controlled through NdhR (category I, completely deregulated). However, a strong TSS was identified upstream of the third gene (*slr2008*), and two independent transcriptional units were defined (Kopf et al., 2014a; Table V). Thus, *slr2006/slr2007* and *slr2008-slr2013* are obviously transcribed as two separate mRNAs, consistent with independent regulation. However, *slr2008* and the downstream genes were also completely derepressed in Δ*ndhR*, despite the fact that the NdhR motif is not present upstream of that cluster. Notably, *slr2006* is the only gene in which the motif overlapped the -10 element and the TSS. Thus, the absence of NdhR might cause an artificial situation involving the free access of RNA polymerase to an obviously strong promoter. Thus, the up-regulation of the downstream transcript (*slr2008-slr2013*) might reflect simple read through from the upstream cluster.

Moreover, we present clear evidence that NdhR might have additional functions or work in cooperation with other regulators, as the expression pattern of

the genes altered in the Δ*ndhR* mutant could be classified into five different categories (Fig. 3). Thereby, only category I genes showed complete deregulation in Δ*ndhR*, likely reflecting the relative position of the binding motif, which is also unique among all categories (see above). Other genes, such as *ndhF3* and *sbtA*, were only partially derepressed in Δ*ndhR* under HC and showed further increases in the mRNA levels in LC-shifted cells. This finding suggests the involvement of an additional regulator of category II genes. One potential candidate is the protein Sll0822, belonging to the cyAbrB family of transcriptional regulators, which regulates the asRNA As1_flv4 (Eisenhut et al., 2012) and is central to the regulation of carbon and nitrogen metabolism (Ishii and Hihara, 2008; Yamauchi et al., 2011). Indeed, the cyAbrB2 protein acts as a regulator of the expression of *ndhF3* and *sbtA* (Lieman-Hurwitz et al., 2009), which may explain the induction of these genes under LC in the *ndhR* mutant (Supplemental Table S2). Consistently, these transcripts show a comparable final abundance in long-term LC-adapted wild-type cells and Δ*ndhR* mutants. Of particular interest are genes belonging to categories IV and V, as the deregulation of these genes suggests a role for NdhR as an activator under HC conditions (category IV) or a repressor under LC conditions (category V). The potential repressor activity of NdhR under LC is supported by evidence that cultures of Δ*ndhR* showed growth defects under LC, but not HC, conditions (Supplemental Fig. S3). This growth phenotype suggests a more important role for NdhR under LC conditions, consistent with the metabolic changes discussed below.

The Mutant Δ*ndhR* Is Preacclimated toward LC under HC Conditions

Consistent with the proposed function of NdhR as a major regulator of Ci supply, the main HCO_3^-- and CO_2-uptake systems are derepressed, at least partially, in the mutant (Table V), indicating a preacclimated state in the Δ*ndhR* strain. Despite the high expression of the Ci transporter in Δ*ndhR* under HC, the Ci affinity of mutant cells was not increased compared with wild-type *Synechocystis* 6803 under HC (data not shown). However, an elevated Ci affinity has been reported for the *ndhR* mutant of *Synechococcus* sp. PCC 7002 under HC conditions (Woodger et al., 2007). Consistent with Wang et al. (2004), we observed that the lack of NdhR-mediated regulation did not lead to the reduced growth of Δ*ndhR* mutants under HC conditions. Largely unchanged metabolome data under HC conditions further indicated that NdhR function is not essentially required under HC conditions. We only observed a slight reduction in the pool sizes of some carbohydrates, which previously showed LC-induced changes in wild-type cells. However, the majority of metabolites and transcripts for the corresponding enzymes were identified at unchanged levels in mutant cells under HC (Supplemental Data Set S2). However, the metabolome data of the short-term response to a sudden LC shift clearly indicated that the successful preacclimation of the Δ*ndhR* mutant also occurred in *Synechocystis* 6803, consistent with globally delayed metabolic responses to the LC shift (Fig. 5A) and the lack or delay of the photorespiratory burst in the mutant (Fig. 6). The photorespiratory burst is characterized by the rapid and transient accumulation of early toxic intermediates, specifically 2PG, glycolate, and Gly, of the photorespiration cycle in wild-type plants. This transient increase in the pool sizes might reflect the sudden activation of the Rubisco oxygenation reaction before the CCM is fully activated in wild-type cells.

Although the Δ*ndhR* mutant is successfully preacclimated to Ci-limiting conditions under HC, a growth defect was also observed under long-term LC conditions (Supplemental Fig. S3; Wang et al., 2004). This finding suggests an important function for NdhR under extended LC, rather than a role in the avoidance of short-term damage (e.g. through rapidly increased photorespiration). In addition to the repressor NdhR, CmpR is a transcriptional activator under LC conditions. Similar to NdhR, CmpR belongs to the large LTTR family (Schell, 1993). The *cmpABCD* operon encoding BCT1 represents the only known target for this protein. The binding of CmpR to the regulatory region is enhanced by the presence of 2PG and RubP (Nishimura et al., 2008). The metabolic photorespiratory burst observed in this study supports the postulated involvement of 2PG in Ci sensing and the regulation of the CCM (Kaplan and Reinhold, 1999; Eisenhut et al., 2008a; Schwarz et al., 2011; Haimovich-Dayan et al., 2014). Specifically, the transient increase of 2PG might induce the expression of the high-affinity HCO_3^- transport system encoded by the *cmpABCD* operon as one of the early acclimation responses to low Ci supply (Omata et al., 1999), while other regulatory processes might act slower. It would be interesting to determine whether CmpR has targets other than the *cmp* operon in *Synechocystis* 6803. Assuming more widespread binding of CmpR, this protein might participate in the LC-mediated regulation of the genes in groups II to V in cooperation with NdhR and/or cyAbrB. In contrast to CmpR, NdhR might play a more important role for the long-term fine-tuning of Ci acquisition systems, as these data indicate that 2OG, the metabolite that activates the repressor NdhR (Daley et al., 2012), belongs to the late-decreasing metabolites (i.e. 2OG was significantly reduced at 24 h after LC shift in wild-type and mutant cells).

Taken together, these data indicate that NdhR and additional metabolites, RNA, and protein factors form a regulation network to ensure complex acclimation to LC conditions. In this network, NdhR not only plays a role as a repressor under HC conditions but also has an important regulatory function under LC conditions. Under these substrate-limiting conditions, it is necessary to achieve the finely tuned expression of the CO_2

and HCO_3^- uptake systems for the optimum balance between acute Ci limitation and the metabolic costs of enhanced Ci acquisition. The growth deficit of Δ*ndhR* under LC might at least partially explain this function of NdhR and NdhR-dependent processes. Obviously, unchecked gene expression is not beneficial; therefore, an imbalance between invested energy and carbon gain is observed in Δ*ndhR* mutants under LC conditions, whereas under the optimal growth conditions of HC, this deregulation is better tolerated in the cell.

MATERIALS AND METHODS

Strains and Growth Conditions

The Glc-tolerant strain *Synechocystis* sp. PCC 6803 was used as the wild type (obtained from N. Murata, National Institute for Basic Biology). Cultures were grown as described before (Schwarz et al., 2011). Briefly, the cells were cultivated under standard conditions in BG11 medium (Rippka et al., 1979) buffered with 20 mM TES-KOH to pH 8 that was sparked with air enriched with 5% (v/v) CO_2 at 29°C and continuous illumination at 120 μmol photons m^{-2} s^{-1}. The mutant Δ*sll1594*::Km (hereafter Δ*ndhR*), in which the gene *sll1594* is disrupted by the insertion of an aminoglycoside phosphotransferase II (*aphII*) gene, was obtained from Teruo Ogawa (Biocenter of the University of Nagoya) and grown in kanamycin-supplemented medium (final concentration, 50 μg mL^{-1}). For CO_2 shift experiments, cells were precultivated with air enriched with 5% (v/v) CO_2 (defined as HC). Then, cells were harvested by centrifugation (5 min at 3,000*g* and 20°C). The pellet was washed and resuspended in fresh BG11 medium of pH 7 at an optical density at 750 nm (OD_{750}) of 0.8. After 1 h of cultivation under HC, CO_2 limitation was set by shifting the exponentially growing cultures to bubbling with ambient air containing 0.040% (v/v) CO_2 (defined as LC). For long-term acclimation to HC or LC, cells were cultivated under the defined conditions for 72 h. The suspensions were diluted daily to OD_{750} = 0.8 by the corresponding medium.

RNA Extraction and Northern Blots

Synechocystis 6803 cells were collected by rapid filtration on hydrophilic polyethersulfone filters (Pall Supor 800 filter; 0.8 μm). Filters with precipitated cells were dissolved in 1 mL of PGTX (Pinto et al., 2009), which has the following composition: 39.6% (w/v) phenol, 7% (v/v) glycerol, 7 mM 8-hydroxyquinoline, 20 mM EDTA, 97.5 mM sodium acetate, 0.8 M guanidine thiocyanate, and 0.48 M guanidine hydrochloride. RNA was extracted as described (Hein et al., 2013). For northern hybridization, RNA was separated on denaturing agarose gels and transferred to Hybond-N^+ nylon membranes (Amersham Scientific) by capillary blotting with 20× SSC buffer. The membranes were hybridized with [α-^{32}P]UTP-incorporated single-stranded RNA probes generated by in vitro transcription as described (Steglich et al., 2008). Signals were detected on a Personal Molecular Imager system (Pharos FX; Bio-Rad) and analyzed with Quantity One software (Bio-Rad).

Microarray Hybridization and Evaluation

For the microarray analysis, RNA was extracted from 5 mL of exponentially growing cultures (OD_{750} of approximately 0.8) harvested by centrifugation (6,000 rpm at 4°C for 10 min). Prior to labeling, 10 μg of total RNA was treated with Turbo DNase (Invitrogen) according to the manufacturer's protocol and precipitated with ethanol/sodium acetate. Labeling and hybridization were performed as described earlier (Georg et al., 2009) using 3 μg of RNA for direct labeling and 1.65 μg of the labeled RNA for hybridization. The microarray hybridization was performed with two biological replicates for each sampling point (except for the 24-h LC sample of Δ*ndhR*, for which triplicates were analyzed). Additionally, the array chip used contained technical replicates for each single probe. Moreover, almost all features are covered by several independent probes. Hence, mean values for all probes of a given feature were used for the final calculation of fold changes. Data processing and statistical evaluation were performed using the R software as described previously (Georg et al., 2009).

The full data set is accessible from the Gene Expression Omnibus database with the accession number GSE63352. In Supplemental Tables S1 and S2, features are separated into mRNAs, asRNAs, ncRNAs, 5′ UTRs, and transcripts derived from internal (within coding sequence) TSSs. However, it should be noted that for every category, overlaps are possible (i.e. the annotation as well as the microarray detection of ncRNAs are often ambiguous because they can overlap with UTRs). Thus, all features labeled in Table IV with the systematic prefix NC are referred to as potentially trans-encoded ncRNAs. For the evaluation presented here, only ncRNAs with an annotation based on Mitschke et al. (2011) were considered.

Generation of Reporter Strains and Luciferase Assays

Luciferase expression was measured as bioluminescence emitted by *Synechocystis* spp. strains carrying transcriptional fusions of the *luxAB* reporter cassette with the upstream sequence of *csiR1*. The putative promoter was amplified from genomic DNA using the oligonucleotides PSyR14_AgeI_fw (5′-tgtaccggtAGGAAATGGGATGTTCCCCCTATC-3′) and PSyR14_FseI_rev (5′-tagaaggccggccCAGTCCCATCCTAGGAAAAATTCC-3′ [the lowercase letters indicate added, noncomplementary sequences containing sites for the restriction enzymes *AgeI* and *FseI* {underlined} that were used for cloning]). The corresponding product was fused to *luxAB* and integrated into the genome of a decanal-producing host strain as described previously (Klähn et al., 2014). Bioluminescence was measured in vivo as total light counts per second from 200 μL of cell suspension using the VICTOR^3 multiplate reader (PerkinElmer). Samples were taken from aerated (LC) liquid cultures as well as after CO_2 enrichment (5%; HC). The data were normalized to OD_{750}.

Metabolome Analysis

Sampling of cells grown under HC or LC conditions was performed by fast filtration in the light and immediate shock freezing in liquid nitrogen (Schwarz et al., 2011). All experiments were repeated three times using independent cell cultures, of which at least two technical replicate samples per culture and condition were taken and analyzed simultaneously. A metabolite fraction enriched for primary metabolites was profiled, and relative pool size changes were determined as described previously (Schwarz et al., 2014), using the established gas chromatography-electron ionization-time of flight-mass spectrometry profiling platform (Eisenhut et al., 2008a). Profiles were analyzed both in a nontargeted approach using all detectable mass features and in a multitargeted approach using the profile data of annotated metabolites only. The determined amounts of mass features and annotated metabolites were normalized to an internal standard, [D-$^{13}C_6$]sorbitol (CAS 121067-66-1; Sigma-Aldrich), which was added to the extraction solvent and normalized to the amount of cell material using the OD_{750} of each sample (Huege et al., 2011). Metabolites were annotated manually by match to the retention index and mass spectral reference data of the Golm Metabolome Database (Hummel et al., 2010). Criteria for positive annotation were the presence of at least three specific mass fragments per compound and a retention index deviation of less than 1% (Strehmel et al., 2008). The relative pool size changes of metabolites are expressed by response ratios (i.e. *x*-fold factors of normalized amounts), comparing all mutant and LC-shifted cells with a single reference condition, namely, the wild type after 24 h at HC.

Metabolite response categories were generated by trend analysis of the wild-type response to the shift from HC to LC. The categories were based on HCA using a Euclidian distance metric and complete linkage. The Ci responsiveness and the deviation of the mutant response compared with wild-type Ci responsiveness (i.e. the Δ*ndhR* responsiveness) of each metabolite were evaluated by two-way ANOVA, Mack-Skillings test, and heteroscedastic Student's *t* test. An ICA of all observed mass features and replicates was performed after $\log_{10}$ transformation and based on the first five components of a preceding principal component analysis using the MetaGeneAlyse Web-based tool (http://metagenealyse.mpimp-golm.mpg.de/). All statistical analyses and HCA were performed using $\log_{10}$-transformed response ratios and averaged technical replicates. For the heteroscedastic Student's *t* test, Microsoft Excel 2010 was used. HCA and other statistical tests were performed using the multiexperiment viewer software MeV, version 4.9 (Saeed et al., 2003).

Supplemental Data

The following supplemental materials are available.

Supplemental Figure S1. Overlap and additional features of the array design used here (Mitschke et al., 2011) with arrays from Wang et al. (2004) and Eisenhut et al. (2007).

Supplemental Figure S2. Overlap and differences in expression levels for protein encoding genes to Wang et al. (2004) under HC conditions.

Supplemental Figure S3. Genotypic and phenotypic characterization of the *Synechocystis* 6803 mutant Δ*ndhR*.

Supplemental Table S1. Complete data set of the transcriptome analysis of wild-type cells of *Synechocystis* sp. PCC 6803.

Supplemental Table S2. Complete data set of the transcriptome analysis of cells of the *Synechocystis* sp. PCC 6803 mutant Δ*ndhR*.

Supplemental Table S3. Antisense-mRNA pairs for which an expression change was observed for the asRNA but not for the corresponding mRNA.

Supplemental Table S4. LC-induced features that are independent from NdhR but whose expression induction appeared delayed.

Supplemental Table S5. Complete data set of the metabolome analysis.

Supplemental Data Set S1. Graphical overview of array signal intensities mapped along the *Synechocystis* chromosome.

Supplemental Data Set S2. Comprehensive view of metabolic and transcriptional changes in the wild type and a Δ*ndhR* mutant of *Synechocystis* 6803 in response to a shift in Ci supply.

ACKNOWLEDGMENTS

We thank Dr. Teruo Ogawa for providing the Δ*ndhR* mutant.

Received November 19, 2014; accepted January 27, 2015; published January 17, 2015.

LITERATURE CITED

Bailey TL, Boden M, Buske FA, Frith M, Grant CE, Clementi L, Ren J, Li WW, Noble WS (2009) MEME SUITE: tools for motif discovery and searching. Nucleic Acids Res **37:** W202–W208

Bauwe H, Hagemann M, Fernie AR (2010) Photorespiration: players, partners and origin. Trends Plant Sci **15:** 330–336

Berner RA (1990) Atmospheric carbon dioxide levels over phanerozoic time. Science **249:** 1382–1386

Carmel D, Dahlström KM, Holmström M, Allahverdiyeva Y, Battchikova N, Aro EM, Salminen TA, Mulo P (2013) Structural model, physiology and regulation of Slr0006 in *Synechocystis* PCC 6803. Arch Microbiol **195:** 727–736

Daley SME, Kappell AD, Carrick MJ, Burnap RL (2012) Regulation of the cyanobacterial CO_2-concentrating mechanism involves internal sensing of $NADP^+$ and α-ketogutarate levels by transcription factor CcmR. PLoS ONE **7:** e41286

Eisenhut M, Aguirre von Wobeser E, Jonas L, Schubert H, Ibelings BW, Bauwe H, Matthijs HCP, Hagemann M (2007) Long-term response toward inorganic carbon limitation in wild type and glycolate turnover mutants of the cyanobacterium *Synechocystis* sp. strain PCC 6803. Plant Physiol **144:** 1946–1959

Eisenhut M, Georg J, Klähn S, Sakurai I, Mustila H, Zhang P, Hess WR, Aro EM (2012) The antisense RNA As1_flv4 in the cyanobacterium *Synechocystis* sp. PCC 6803 prevents premature expression of the *flv4-2* operon upon shift in inorganic carbon supply. J Biol Chem **287:** 33153–33162

Eisenhut M, Huege J, Schwarz D, Bauwe H, Kopka J, Hagemann M (2008a) Metabolome phenotyping of inorganic carbon limitation in cells of the wild type and photorespiratory mutants of the cyanobacterium *Synechocystis* sp. strain PCC 6803. Plant Physiol **148:** 2109–2120

Eisenhut M, Ruth W, Haimovich M, Bauwe H, Kaplan A, Hagemann M (2008b) The photorespiratory glycolate metabolism is essential for cyanobacteria and might have been conveyed endosymbiontically to plants. Proc Natl Acad Sci USA **105:** 17199–17204

Figge RM, Cassier-Chauvat C, Chauvat F, Cerff R (2001) Characterization and analysis of an NAD(P)H dehydrogenase transcriptional regulator critical for the survival of cyanobacteria facing inorganic carbon starvation and osmotic stress. Mol Microbiol **39:** 455–468

Georg J, Dienst D, Schürgers N, Wallner T, Kopp D, Stazic D, Kuchmina E, Klähn S, Lokstein H, Hess WR, et al (2014) The small regulatory RNA SyR1/PsrR1 controls photosynthetic functions in cyanobacteria. Plant Cell **26:** 3661–3679

Georg J, Hess WR (2011) cis-Antisense RNA, another level of gene regulation in bacteria. Microbiol Mol Biol Rev **75:** 286–300

Georg J, Voss B, Scholz I, Mitschke J, Wilde A, Hess WR (2009) Evidence for a major role of antisense RNAs in cyanobacterial gene regulation. Mol Syst Biol **5:** 305

Goethals K, Van Montagu M, Holsters M (1992) Conserved motifs in a divergent nod box of *Azorhizobium caulinodans* ORS571 reveal a common structure in promoters regulated by LysR-type proteins. Proc Natl Acad Sci USA **89:** 1646–1650

Hackenberg C, Huege J, Engelhardt A, Wittink F, Laue M, Matthijs HCP, Kopka J, Bauwe H, Hagemann M (2012) Low-carbon acclimation in carboxysome-less and photorespiratory mutants of the cyanobacterium *Synechocystis* sp. strain PCC 6803. Microbiology **158:** 398–413

Hackenberg C, Kern R, Hüge J, Stal LJ, Tsuji Y, Kopka J, Shiraiwa Y, Bauwe H, Hagemann M (2011) Cyanobacterial lactate oxidases serve as essential partners in N_2 fixation and evolved into photorespiratory glycolate oxidases in plants. Plant Cell **23:** 2978–2990

Haimovich-Dayan M, Lieman-Hurwitz J, Orf I, Hagemann M, Kaplan A (2014) Does 2-phosphoglycolate serve as an internal signal molecule of inorganic carbon deprivation in the cyanobacterium *Synechocystis* sp. PCC 6803? Environ Microbiol **17:** 1794–1804

Hein S, Scholz I, Voß B, Hess WR (2013) Adaptation and modification of three CRISPR loci in two closely related cyanobacteria. RNA Biol **10:** 852–864

Huege J, Goetze J, Schwarz D, Bauwe H, Hagemann M, Kopka J (2011) Modulation of the major paths of carbon in photorespiratory mutants of *Synechocystis*. PLoS ONE **6:** e16278

Hummel J, Strehmel N, Selbig J, Walther D, Kopka J (2010) Decision tree supported substructure prediction of metabolites from GC-MS profiles. Metabolomics **6:** 322–333

Husic DW, Husic HD, Tolbert NE, Black CC (1987) The oxidative photosynthetic carbon cycle or C2 cycle. Crit Rev Plant Sci **5:** 45–100

Ishii A, Hihara Y (2008) An AbrB-like transcriptional regulator, Sll0822, is essential for the activation of nitrogen-regulated genes in *Synechocystis* sp. PCC 6803. Plant Physiol **148:** 660–670

Kaniya Y, Kizawa A, Miyagi A, Kawai-Yamada M, Uchimiya H, Kaneko Y, Nishiyama Y, Hihara Y (2013) Deletion of the transcriptional regulator cyAbrB2 deregulates primary carbon metabolism in *Synechocystis* sp. PCC 6803. Plant Physiol **162:** 1153–1163

Kaplan A, Reinhold L (1999) CO_2 concentrating mechanisms in photosynthetic microorganisms. Annu Rev Plant Physiol Plant Mol Biol **50:** 539–570

Kelly GJ, Latzko E (1977) Chloroplast phosphofructokinase: II. Partial purification, kinetic and regulatory properties. Plant Physiol **60:** 295–299

Klähn S, Baumgartner D, Pfreundt U, Voigt K, Schön V, Steglich C, Hess WR (2014) Alkane biosynthesis genes in cyanobacteria and their transcriptional organization. Front Bioeng Biotechnol **2:** 24

Kopf M, Klähn S, Scholz I, Hess WR, Voss B (2015) Variations in the noncoding transcriptome as a driver of inter-strain divergence and physiological adaptation in bacteria. Sci Rep **5:** 9560

Kopf M, Klähn S, Scholz I, Matthiessen JKF, Hess WR, Voß B (2014a) Comparative analysis of the primary transcriptome of *Synechocystis* sp. PCC 6803. DNA Res **21:** 527–539

Kopf M, Klähn S, Voss B, Stüber K, Huettel B, Reinhardt R, Hess WR (2014b) Finished genome sequence of the unicellular cyanobacterium Synechocystis sp. strain PCC 6714. Genome Announc **2:** e00757-14

Lieman-Hurwitz J, Haimovich M, Shalev-Malul G, Ishii A, Hihara Y, Gaathon A, Lebendiker M, Kaplan A (2009) A cyanobacterial AbrB-like protein affects the apparent photosynthetic affinity for CO_2 by modulating low-CO_2-induced gene expression. Environ Microbiol **11:** 927–936

Maddocks SE, Oyston PCF (2008) Structure and function of the LysR-type transcriptional regulator (LTTR) family proteins. Microbiology **154:** 3609–3623

Mitschke J, Georg J, Scholz I, Sharma CM, Dienst D, Bantscheff J, Voss B, Steglich C, Wilde A, Vogel J, et al (2011) An experimentally

anchored map of transcriptional start sites in the model cyanobacterium *Synechocystis* sp. PCC6803. Proc Natl Acad Sci USA **108:** 2124–2129

Narikawa R, Suzuki F, Yoshihara S, Higashi S, Watanabe M, Ikeuchi M (2011) Novel photosensory two-component system (PixA-NixB-NixC) involved in the regulation of positive and negative phototaxis of cyanobacterium *Synechocystis* sp. PCC 6803. Plant Cell Physiol **52:** 2214–2224

Nishimura T, Takahashi Y, Yamaguchi O, Suzuki H, Maeda S, Omata T (2008) Mechanism of low CO_2-induced activation of the *cmp* bicarbonate transporter operon by a LysR family protein in the cyanobacterium *Synechococcus elongatus* strain PCC 7942. Mol Microbiol **68:** 98–109

Norman EG, Colman B (1991) Purification and characterization of phosphoglycolate phosphatase from the cyanobacterium *Coccochloris peniocystis*. Plant Physiol **95:** 693–698

Ochoa de Alda JAG, Esteban R, Diago ML, Houmard J (2014) The plastid ancestor originated among one of the major cyanobacterial lineages. Nat Commun **5:** 4937

Omata T, Gohta S, Takahashi Y, Harano Y, Maeda S (2001) Involvement of a CbbR homolog in low CO_2-induced activation of the bicarbonate transporter operon in cyanobacteria. J Bacteriol **183:** 1891–1898

Omata T, Price GD, Badger MR, Okamura M, Gohta S, Ogawa T (1999) Identification of an ATP-binding cassette transporter involved in bicarbonate uptake in the cyanobacterium *Synechococcus* sp. strain PCC 7942. Proc Natl Acad Sci USA **96:** 13571–13576

Pinto FL, Thapper A, Sontheim W, Lindblad P (2009) Analysis of current and alternative phenol based RNA extraction methodologies for cyanobacteria. BMC Mol Biol **10:** 79

Price GD, Badger MR, Woodger FJ, Long BM (2008) Advances in understanding the cyanobacterial CO_2-concentrating-mechanism (CCM): functional components, Ci transporters, diversity, genetic regulation and prospects for engineering into plants. J Exp Bot **59:** 1441–1461

Rippka R, Deruelles J, Waterbury JB, Herdman M, Stanier RY (1979) Generic assignments, strain histories and properties of pure cultures of cyanobacteria. J Gen Microbiol **111:** 1–61

Saeed AI, Sharov V, White J, Li J, Liang W, Bhagabati N, Braisted J, Klapa M, Currier T, Thiagarajan M, et al (2003) TM4: a free, open-source system for microarray data management and analysis. Biotechniques **34:** 374–378

Sakurai I, Stazic D, Eisenhut M, Vuorio E, Steglich C, Hess WR, Aro EM (2012) Positive regulation of *psbA* gene expression by cis-encoded antisense RNAs in *Synechocystis* sp. PCC 6803. Plant Physiol **160:** 1000–1010

Schell MA (1993) Molecular biology of the LysR family of transcriptional regulators. Annu Rev Microbiol **47:** 597–626

Schwarz D, Nodop A, Hüge J, Purfürst S, Forchhammer K, Michel KP, Bauwe H, Kopka J, Hagemann M (2011) Metabolic and transcriptomic phenotyping of inorganic carbon acclimation in the cyanobacterium *Synechococcus elongatus* PCC 7942. Plant Physiol **155:** 1640–1655

Schwarz D, Orf I, Kopka J, Hagemann M (2013) Recent applications of metabolomics toward cyanobacteria. Metabolites **3:** 72–100

Schwarz D, Orf I, Kopka J, Hagemann M (2014) Effects of inorganic carbon limitation on the metabolome of the *Synechocystis* sp. PCC 6803 mutant defective in *glnB* encoding the central regulator PII of cyanobacterial C/N acclimation. Metabolites **4:** 232–247

Shibata M, Ohkawa H, Kaneko T, Fukuzawa H, Tabata S, Kaplan A, Ogawa T (2001) Distinct constitutive and low-CO_2-induced CO_2 uptake systems in cyanobacteria: genes involved and their phylogenetic relationship with homologous genes in other organisms. Proc Natl Acad Sci USA **98:** 11789–11794

Singh AK, Sherman LA (2002) Characterization of a stress-responsive operon in the cyanobacterium *Synechocystis* sp. strain PCC 6803. Gene **297:** 11–19

Song JY, Cho HS, Cho JI, Jeon JS, Lagarias JC, Park YI (2011) Near-UV cyanobacteriochrome signaling system elicits negative phototaxis in the cyanobacterium *Synechocystis* sp. PCC 6803. Proc Natl Acad Sci USA **108:** 10780–10785

Steglich C, Futschik ME, Lindell D, Voss B, Chisholm SW, Hess WR (2008) The challenge of regulation in a minimal photoautotroph: noncoding RNAs in *Prochlorococcus*. PLoS Genet **4:** e1000173

Strehmel N, Hummel J, Erban A, Strassburg K, Kopka J (2008) Retention index thresholds for compound matching in GC-MS metabolite profiling. J Chromatogr B Analyt Technol Biomed Life Sci **871:** 182–190

Stuart BJ (2011) Addressing the grand challenge of atmospheric carbon dioxide: geologic sequestration vs. biological recycling. J Biol Eng **5:** 14

Wang HL, Postier BL, Burnap RL (2004) Alterations in global patterns of gene expression in *Synechocystis* sp. PCC 6803 in response to inorganic carbon limitation and the inactivation of *ndhR*, a LysR family regulator. J Biol Chem **279:** 5739–5751

Woodger FJ, Bryant DA, Price GD (2007) Transcriptional regulation of the CO_2-concentrating mechanism in a euryhaline, coastal marine cyanobacterium, *Synechococcus* sp. strain PCC 7002: role of NdhR/CcmR. J Bacteriol **189:** 3335–3347

Yamauchi Y, Kaniya Y, Kaneko Y, Hihara Y (2011) Physiological roles of the cyAbrB transcriptional regulator pair Sll0822 and Sll0359 in *Synechocystis* sp. strain PCC 6803. J Bacteriol **193:** 3702–3709

Young JD, Shastri AA, Stephanopoulos G, Morgan JA (2011) Mapping photoautotrophic metabolism with isotopically nonstationary ^{13}C flux analysis. Metab Eng **13:** 656–665

Zhang P, Eisenhut M, Brandt AM, Carmel D, Silén HM, Vass I, Allahverdiyeva Y, Salminen TA, Aro EM (2012) Operon *flv4-flv2* provides cyanobacterial photosystem II with flexibility of electron transfer. Plant Cell **24:** 1952–1971